

Stable multispeed lattice Boltzmann methods

R. A. Brownlee,* A. N. Gorban, and J. Levesley

Department of Mathematics, University of Leicester, Leicester LE1 7RH, UK

(Dated: February 6, 2008)

We demonstrate how to produce a stable multispeed lattice Boltzmann method (LBM) for a wide range of velocity sets, many of which were previously thought to be intrinsically unstable. We use non-Gauss–Hermitian cubatures. The method operates stably for almost zero viscosity, has second-order accuracy, suppresses typical spurious oscillation (only a modest Gibbs effect is present) and introduces no artificial viscosity. There is almost no computational cost for this innovation.

DISCLAIMER: Additional tests and wide discussion of this preprint show that the claimed property of coupled steps: no artificial dissipation and the second-order accuracy of the method are valid only on sufficiently fine grids. For coarse grids the higher-order terms destroy coupling of steps and additional dissipation appears.

The equations are true.

I. INTRODUCTION

The lattice Boltzmann method (LBM) is a discrete velocity method primarily used in the numerical simulation of complex fluid problems. The essence of the method is that a finite number of populations stream and collide on a fixed computational lattice in such a manner that their populations' velocity moments obey the Navier–Stokes equations.

There are a number of ways to derive the method [1]. Historically, the method comes from lattice gas automata theory but it can also be derived directly by the overrelaxation discretization of Boltzmann's kinetic transport equation.

We prefer to describe the LBM without direct reference to Boltzmann's equation. Indeed, we prefer to describe the LBM as being generated wholly by the mechanical motion, of a single-particle distribution function, by free-flight and entropic involution. In this setting, the LBM is the discrete dynamical system which arises by discretizing this motion in a particular manner. The discrete velocity set arises as approximation nodes of certain cubature in velocity space [2], where these nodes are automorphisms of some underlying lattice.

A consequence of this realisation is that the stability analysis (and analysis of conservation laws) of the LBM is more natural. One is able to clearly identify the main instability mechanisms of the LBM (Sect. II), which are triggered when the continuous mechanical motion of free-flight and entropic involution is discretized.

A further consequence of viewing the LBM in this setting (also in Sect. II) is that a prescription of coupled steps is suggested to stabilise the method. After proceeding for one step of the usual overrelaxation LBM scheme (LBGK), populations are streamed and then replaced with their local equilibrium distribution. Additional dissipation results but the scheme retains the second-order in time accuracy of LBGK. Compared with the standard LBM, the proposed scheme of coupled steps constitutes

no additional computational cost.

Each cubature rule gives rise to its own LBM, and multispeed lattice schemes can be readily concocted (Sect. III). Multispeed lattices are an attractive prospect because they promise greater flexibility in the attainable sound speed provided by the model, allow for the modelling of nonisothermic flows and the dynamics of higher moments as well. The literature sometimes contains statements whose sentiment is that some multispeed lattice LBM schemes are inherently numerically unstable (see, e.g., [3, 4]). On the contrary, we observe that the aforementioned LBM of coupled steps is stable for a variety of multispeed lattices and we demonstrate this through the numerical simulation of a one-dimensional isothermal shock tube (Sect. IV).

II. THE LATTICE BOLTZMANN METHOD

To describe the LBM as being generated by free-flight and entropic involution requires a certain amount of background knowledge and terminology which we now briefly introduce. For proofs and further justification of any statements, the reader should consult [2, 6]. The free-flight equation is given by

$$\frac{\partial f}{\partial t} + \mathbf{v} \cdot \nabla f = 0, \quad (1)$$

where $f = f(\mathbf{x}, \mathbf{v}, t)$ is a single-particle distribution function, \mathbf{x} is the space vector, \mathbf{v} is velocity. This equation preserves the value of a strictly concave entropy functional, $S(f)$. The default choice of entropy is

$$S(f) = - \int f \log f \, d\mathbf{v} d\mathbf{x}. \quad (2)$$

In addition, we have a fixed linear mapping $m : f \mapsto M$ to some macroscopic variables. For example, in hydrodynamic applications M is the vector of five hydrodynamic fields $(n, n\mathbf{u}, E)$ (density–momentum–energy):

$$n := \int f \, d\mathbf{v}, \quad n\mathbf{u}_j := \int v_j f \, d\mathbf{v}, \quad E := \frac{1}{2} \int \mathbf{v}^2 f \, d\mathbf{v}. \quad (3)$$

*corresponding author: r.brownlee@mcs.le.ac.uk

For each M , the *quasiequilibrium state* f_M^* is defined as the unique solution of the constrained optimisation problem: $\arg \max\{S(f) : m(f) = M\}$. For the hydrodynamic fields $M = M(\mathbf{x}, t)$ (3), the quasiequilibrium state is the well known local Maxwellian

$$f_M^*(\mathbf{v}) = n \left(\frac{2\pi k_B T}{m} \right)^{-3/2} \exp \left(-\frac{m(\mathbf{v} - \mathbf{u})^2}{2k_B T} \right). \quad (4)$$

where m is particle mass, k_B is Boltzmann's constant and T is kinetic temperature.

For every f , a corresponding quasiequilibrium state $f_{m(f)}^*$ is defined. The set of all quasiequilibrium states is parameterised by the macroscopic variables, M , and defines the *quasiequilibrium manifold*, which we denote by \mathbf{q}_0 .

The quasiequilibrium approximation for the free-flight equation (1) is the following evolution equation for the macroscopic variables

$$\frac{dM}{dt} = -m(\mathbf{v} \cdot \nabla(f_M^*)). \quad (5)$$

For the hydrodynamics fields (3) the system (5) is the compressible Euler equations.

We denote by Π_S the projector of a point f onto \mathbf{q}_0 : $\Pi_S : f \mapsto f_{m(f)}^*$. Let Θ_t be the time shift transformation for the free-flight equation (1): $\Theta_t : f(\mathbf{x}, \mathbf{v}) \mapsto f(\mathbf{x} - \mathbf{v}t, \mathbf{v})$. Now, for a fixed time step τ , the following step provides a second-order in time step τ approximation to the solution of the conservative macroscopic equations (5):

$$\begin{aligned} M(0) &= m(\Pi_S(\Theta_{-\tau/2}(f_M^*))) \\ &\mapsto m(\Pi_S(\Theta_{\tau/2}(f_M^*))) = M(\tau). \end{aligned} \quad (6)$$

If we would like to model dissipative dynamics then we should follow the free-flight trajectory by some extra time $\varsigma \leq \tau$:

$$\begin{aligned} M(0) &= m(\Pi_S(\Theta_{-\vartheta/2}(f_M^*))) \\ &\mapsto m(\Pi_S(\Theta_{\varsigma+\vartheta/2}(f_M^*))) = M(\varsigma + \vartheta) = M(\tau), \end{aligned} \quad (7)$$

where $\vartheta = \tau - \varsigma$. Now, (7) provides a second-order in time step τ approximation to the solution of the compressible Navier–Stokes equations with dynamic viscosity $\mu = \frac{\varsigma}{2}P$ and Prandtl number $Pr = 1$.

Equations (6) and (7) constitute one step of an approximation to some conservative and dissipative macroscopic equations, respectively. To iterate and produce a step wise approximation to the macroscopic equations for time greater than τ we can employ (*partial*) *entropic involution*.

It will be useful to define the *film of nonequilibrium states* [2, 7, 8] as the manifold \mathbf{q} that is the trajectory (forward and backward in time) of the quasiequilibrium manifold. A point $f \in \mathbf{q}$ is naturally parameterised by (M, τ) : $f = q_{M, \tau}$, where $M = m(f)$ is the value of the macroscopic variables, and $\tau = \tau(f)$ is the time shift from

a quasiequilibrium state: $\Theta_{-\tau}(f)$ is a quasiequilibrium state for some (other) value of M . The quasiequilibrium manifold divides \mathbf{q} into two parts, $\mathbf{q} = \mathbf{q}_- \cup \mathbf{q}_0 \cup \mathbf{q}_+$, where $\mathbf{q}_- = \{q_{M, \tau} | \tau < 0\}$ and $\mathbf{q}_+ = \{q_{M, \tau} | \tau > 0\}$.

Now, the *partial entropic involution* operator I_S^β is defined as follows: for $f \in \mathbf{q}_\pm$ the point $g = I_S^\beta(f) \in \mathbf{q}_\mp$, for $\beta \in [1/2, 1)$, is specified by the two conditions:

$$\begin{aligned} m(g) &= m(f), \\ S(g) - S(\Pi_S(f)) &= (2\beta - 1)^2(S(f) - S(\Pi_S(f))). \end{aligned}$$

If $\beta = 1$ in this definition we refer to the operator as *entropic involution* and denote it by I_S . The point $I_S^\beta(f)$, $\beta \in [1/2, 1)$, is closer to the quasiequilibrium point $\Pi_S(f)$ (with respect to entropy) than $I_S(f)$.

If $f_0 \in \mathbf{q}_0$, then, after some initial steps, the following sequence gives a second-order in time step τ approximation of the compressible Navier–Stokes equations (as mentioned above) with $\varsigma = (1 - \beta)\tau/\beta$, $\beta \in [1/2, 1)$:

$$M(n\tau) = m((I_S^\beta \Theta_\tau)^n f_0), \quad n = 0, 1, \dots \quad (8)$$

For entropic involution ($\beta = 1$), (8) provides a second-order in time step τ approximation of the compressible Euler equations with time step 2τ .

Finally, to generate the standard LBM we must perform three tasks:

1. transfer to a finite number of velocities with the same macroscopic equations;
2. transfer from space to a lattice, where these velocities are automorphisms;
3. transfer from dynamics and involution on \mathbf{q} to the whole space of states.

The first two points will be addressed in Sect. II C and Sect. III. To address the final point we replace the operator I_S^β with the transformation

$$I_0^\beta : f \mapsto \Pi_S(f) + (2\beta - 1)(\Pi_S(f) - f). \quad (9)$$

If, for a given $f_0 \in \mathbf{q}_0$, the sequence (8) gives the sought after second-order in time step τ approximation of the macroscopic equations, then the sequence

$$M(n\tau) = m((I_0^\beta \Theta_\tau)^n f_0), \quad n = 0, 1, \dots, \quad (10)$$

also gives a second-order approximation to the same equations.

A. Instability mechanisms

There are a number of sources of instability which are triggered when the operator I_S^β is replaced with I_0^β (9). Indeed, we identify three main instability mechanisms.

Firstly, a small shift in f in the direction of the vector $f - \Pi_S(f)$ does not relax back for $\beta = 1$, and its relaxation

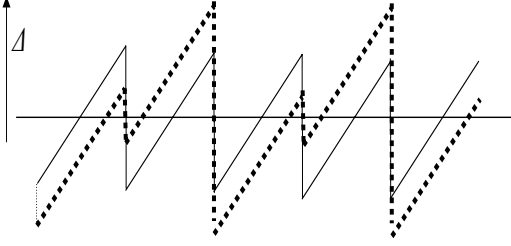


FIG. 1: Neutral stability and one-step oscillations in a sequence successive entropic involutions. Bold dotted line – a perturbed motion, Δ – direction of neutral stability.

is very slow for $\beta \sim 1$ (i.e., for small viscosity). This effect is most easily illustrated by Fig. 1, where a perturbed chain of entropic involutions is shown. This instability, which we refer to as *neutral instability*, causes one step oscillations to be triggered.

Secondly, there is a *nonlinear instability* due to the nonlinear nature of the projector Π_S . More specifically, for all of the accuracy estimates in the previous section, we implicitly use the assumption that f is sufficiently close to q_0 . The sequences (8) and (10) give the same accuracy as one another, but a long chain of steps with the linearised operator I_0^β (9) can lead far from the quasiequilibrium manifold q_0 and even from q itself.

Finally, there is a *directional instability* that can affect accuracy. There can be large deviation in the angle the vector $f - \Pi_S(f)$ makes with the tangent space to q . The directional instability changes the structure of dissipation terms in the target macroscopic equations: accuracy is decreased to the first-order in τ and significant fluctuations of the Prandtl number and viscosity coefficient may occur.

B. Stabilisation

There is a strikingly simple prescription that simultaneously alleviates the effect of all three instabilities identified in the previous section.

Consider starting from a point $f_0 \in q_0$, then evolve the state by Θ_τ and apply the operator I_0^β (9), as is usual. Then, evolve by Θ_τ again and project back on to q_0 using Π_S :

$$M(0) = m(f_0) \mapsto m(\Pi_S(\Theta_\tau(I_0^\beta(\Theta_\tau(f_0)))))) = M(2\tau). \quad (11)$$

This *coupled step* with quasiequilibrium ends is illustrated in Fig. 2 and gives a second-order in time τ approximation, to the shift in time 2τ , for the target macroscopic equations with $\varsigma = 2(1 - \beta)\tau$, $\beta \in [1/2, 1]$. The procedure of periodically restarting from the quasiequilibrium manifold introduces additional dissipation of order τ^2 , and the perturbation of accuracy is of order τ^3 . Hence, the method has the second-order accuracy.

The user should take into account that ς significantly depends on the chain construction. For the sequence (8)

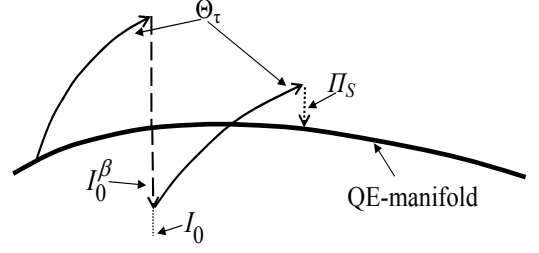


FIG. 2: The scheme of coupled steps with quasiequilibrium ends (11).

we have $\varsigma = (1 - \beta)\tau/\beta$, and for the sequence of steps (11) we have $\varsigma = 2(1 - \beta)\tau$. The viscosity coefficient is proportional to ς . If $1 - \beta$ is small, the coupled step (11) gives around two times larger viscosity than (8).

The result of restarting from q_0 is that the aforementioned neutral instability is obliterated and the effects of nonlinear and directional instabilities are entirely marginalised.

C. Entropy, energy and equilibrium

Many specific forms of entropy for LBMs have been discussed in the literature. There exist two methods of construction: from the Boltzmann entropy approximation to equilibrium (for given macroscopic variables), and from the equilibrium approximation to the Boltzmann entropy approximation. For the latter, the universal entropy formula for a discrete distribution $f = (f_i)$ is the Kullback entropy

$$S_K(f) = - \sum_i f_i \log \left(\frac{f_i}{f_{m(f),i}^*} \right), \quad (12)$$

where f_M^* is the quasiequilibrium distribution parameterised by M . It is trivial to check that $f_M^* = \arg \max \{S_K(f) : m(f) = M\}$. The entropic involution conserves the values of all elements of M . Hence, for energy conservation it is sufficient to have energy inside M (the distributions f and $f_{m(f)}^*$ should have the same energy). In this sense, the long standing problem of energy conservation in LBMs has an obvious and physically meaningful solution (see an example of such a solution in [10]). The classical physical sense of (12) is a nonequilibrium extension of a Massieu–Planck–Kramers function (or grand canonical potential) for a given set of macroscopic variables M .

A constructive approach to choose discrete S and f_M^* is: we use the classical (continuous) quasi-equilibrium distributions and cubature rules to get the appropriate discrete approximation. Then, the entropy that we need for self-consistency of our construction is given by (12).

III. CUBATURE AND MULTISPEED LATTICES

To complete the realisation of the LBM, configuration space is discretized by selecting a finite number of velocities $\{\mathbf{v}_1, \mathbf{v}_2, \dots, \mathbf{v}_\ell\}$. More specifically, for a fixed time step τ , the space discretization will consist of a lattice \mathcal{L} for which the velocities $\mathbf{v}_i\tau$ are automorphisms. Choosing to discretize in this manner means that no spatial discretization error is committed when the continuous free-flight equations

$$\frac{\partial f_i}{\partial t} + \mathbf{v}_i \cdot \nabla f = 0, \quad i = 1, \dots, \ell,$$

are integrated for time τ and evaluated on \mathcal{L} . Here, f_i denotes a single-particle distribution function associated with the velocity \mathbf{v}_i . Note that all of the discretization error is contained in the selection of the discrete velocities.

For hydrodynamics it remains to evaluate the integral moments (3). By construction, the integrals (3) remain unchanged under the substitution of f with the quasiequilibrium state f_M^* (4). Our approach will be to construct cubature rules based upon reproduction of low degree polynomials using the discrete velocities, \mathbf{v}_i , as abscissas. We replace the quasiequilibrium state (4) with its second-order Taylor expansion in \mathbf{u} with terms involving \mathbf{u}^2 and higher disregarded. We denote this polynomial by $p_M^* = p_M^*(\mathbf{v})$, and demand that its first few moments are evaluated exactly by the cubature rule. Another approach, which we do not pursue here, is to employ a discrete version of the entropy (2) from the outset (see, e.g., [9]).

Let us concern ourselves with modelling the isothermal Navier–Stokes equations for the remainder of the paper and set $C^2 = 2k_B T/m$. The “sound speed” of the model is c_s where $c_s^2 = C^2/2$. For the isothermal model we should at least consider all moments up to the third-order, which is equivalent to finding the cubature weights w_i such that

$$\int \mathbf{v}^k \exp\left(-\frac{\mathbf{v}^2}{C^2}\right) d\mathbf{v} \equiv \sum_{i=1}^{\ell} w_i \mathbf{v}_i^k \exp\left(-\frac{\mathbf{v}_i^2}{C^2}\right),$$

for $k = 0, 1, 2, 3$. Using this cubature, the discrete hydrodynamic moments are given by the expressions

$$n = \sum_i f_i, \quad n\mathbf{u} = \sum_i \mathbf{v}_i f_i, \quad E = \frac{1}{2} \sum_i \mathbf{v}_i^2 f_i,$$

where $f_i = f_i(\mathbf{x}, t) := w_i f(\mathbf{x}, \mathbf{v}_i, t)$. The LBM realisation of (8) is then

$$f_i(\mathbf{x} + \mathbf{v}_i\tau, t + \tau) = f_i^* + (2\beta - 1)(f_i^* - f_i), \quad (13)$$

where $f_i^* = f_i^*(\mathbf{x}, t) := w_i p_M^*(\mathbf{v}_i)$. The name often given to (13) in the literature is LBGK. The prescribed scheme of coupled steps (11) is:

$$f_i(\mathbf{x} + \mathbf{v}_i\tau, t + \tau) = \begin{cases} f_i^*, & N_{\text{step}} \text{ odd,} \\ f_i^* + (2\beta - 1)(f_i^* - f_i), & \text{otherwise,} \end{cases} \quad (14)$$

Method	Order	\mathbf{v}_i	W_i	c_s
G–H	5	$\{0, \pm 1\}$	$\{\frac{2}{3}, \frac{1}{6}\}$	$1/\sqrt{3}$
N–C	4	$\{0, \pm 1, \pm 2\}$	$\{\frac{9}{16}, \frac{5}{24}, \frac{1}{96}\}$	$1/\sqrt{2}$
N–C	4	$\{0, \pm 1, \pm 2\}$	$\{\frac{1}{2}, \frac{1}{6}, \frac{1}{12}\}$	1
N–C	4	$\{0, \pm 1, \pm 3\}$	$\{\frac{19}{36}, \frac{15}{64}, \frac{1}{576}\}$	$1/\sqrt{2}$
N–C	4	$\{0, \pm 1, \pm 3\}$	$\{\frac{2}{9}, \frac{3}{8}, \frac{1}{72}\}$	1
N–C	4	$\{0, \pm 1, \pm 4\}$	$\{\frac{33}{64}, \frac{29}{120}, \frac{1}{1920}\}$	$1/\sqrt{2}$
N–C	4	$\{0, \pm 1, \pm 4\}$	$\{\frac{1}{8}, \frac{13}{30}, \frac{1}{240}\}$	1
N–C	6	$\{0, \pm 1, \pm 2, \pm 3\}$	$\{\frac{161}{288}, \frac{27}{128}, \frac{3}{320}, \frac{1}{5760}\}$	$1/\sqrt{2}$
N–C	6	$\{0, \pm 1, \pm 2, \pm 3\}$	$\{\frac{7}{18}, \frac{1}{4}, \frac{1}{20}, \frac{1}{180}\}$	1

TABLE I: Various 1D lattices and weights using different quadratures: G–H means Gauss–Hermite, N–C means Newton–Cotes. The second column shows the order of the moment which is exactly evaluated by the quadrature rule. The final column gives the lattice “sound speed”.

where N_{step} is the cumulative number of time steps taken in the simulation.

Clearly, each set (\mathbf{v}_i, w_i) of velocities and associated cubature weights will define its own LBM.

One way to handle the multivariate case is to use tensor and algebraic products of one-dimensional velocities and weights, respectively. Let us therefore restrict our discussion to one space dimension.

One particular choice of quadrature is Gauss–Hermite quadrature. Indeed, the three-point Gauss–Hermite rule (which exactly evaluates the fifth order moment) is popular [11, 12]. However, the use of multispeed lattices (lattices with more than two non-zero speeds in one-dimension) using higher-order Gauss–Hermite quadrature is precluded because the zeros of the Hermite polynomials, for degree greater than 3, can not be aligned with any regular lattice.

An alternative to Gauss–Hermite is to use Newton–Cotes quadrature which has the advantage that the velocities can be aligned with a lattice before determining the quadrature weights. Multispeed lattices can be readily constructed. For example, suppose we want to employ 5 symmetric quadrature nodes $\{\mathbf{v}_0, \dots, \mathbf{v}_4\} := \{0, \pm aC, \pm bC\}$. Then, $w_i = CW_i\sqrt{\pi} \exp(\mathbf{v}_i^2/C^2)$, where

$$W_0 = \frac{4a^2b^2 - 2a^2 - 2b^2 + 3}{4a^2b^2},$$

$$W_1 = W_2 = \frac{2b^2 - 3}{8(b^2 - a^2)a^2}, \quad W_3 = W_4 = \frac{2a^2 - 3}{8(a^2 - b^2)b^2}.$$

For five distinct nodes we should have $0 < a < b$ but there should be further restrictions on a and b to ensure all weights are positive.

A selection of different quadrature rules are collected in Table I along with their respective lattice “sound speeds”.

IV. NUMERICAL EXPERIMENT

The 1D shock tube for a compressible isothermal fluid is a standard benchmark test for hydrodynamic codes.

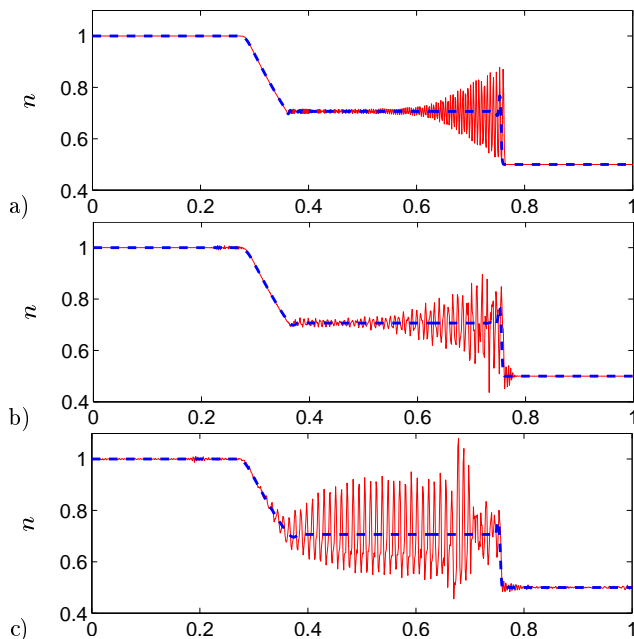


FIG. 3: Density profile of a 1D isothermal shock tube simulation after $100\sqrt{3}/c_s$ time steps using LBGK (solid line) and the coupled steps (14) (dashed line) with the lattice a) $(\mathbf{v}_i, W_i, c_s) = (\{0, \pm 1\}, \{\frac{2}{3}, \frac{1}{6}\}, 1/\sqrt{3})$; b) $(\mathbf{v}_i, W_i, c_s) = (\{0, \pm 1, \pm 2\}, \{\frac{9}{16}, \frac{5}{24}, \frac{1}{96}\}, 1/\sqrt{2})$; c) $(\mathbf{v}_i, W_i, c_s) = (\{0, \pm 1, \pm 2, \pm 3\}, \{\frac{7}{18}, \frac{1}{4}, \frac{1}{20}, \frac{1}{180}\}, 1)$

We will fix the kinematic viscosity of the fluid at $\nu = 10^{-9}$. Our computational domain will be the interval $[0, 1]$ and we discretize this interval with 801 uniformly spaced lattice sites. We choose the initial density ratio as 1:2 so that for $x \leq 400$ we set $n = 1.0$ else we set $n = 0.5$.

In all of our simulations we use a lattice with unit spacing, a unit time step and we have chosen to consider the three-velocity Gauss-Hermite model, as well as five- and seven-velocity Newton-Cotes models (see Fig. 3 for the specific lattices details).

The standard three-velocity LBGK discretization (13) is violently oscillatory in the immediate neighbourhood of the shock, the effects of which extend over much of the domain. The situation is worse for LBGK with five- and seven-velocities; here the oscillations do not remain bounded (we always implement the positivity rule [5, 6] that prohibits negative densities). The scheme quickly becomes meaningless. In comparison, we find that the

proposed scheme of coupled steps (14) gives stable behaviour on all tested lattices, by which we mean no blow-up and spurious post-shock oscillations are observed. In all cases we do observe a small deviation near the shock front which may be an unavoidable Gibbs effect. The amplitude of the Gibbs effect in our experiments decreases by increasing the degree of approximation.

V. CONCLUSIONS

By considering a realisation in which the LBM is wholly generated by free-flight and entropic involution, we have suggested a simple stabilisation procedure of coupled steps (8) which retains the second-order accuracy of the method without artificial viscosity at that order.

The procedure effectively constitutes no additional computational cost and can be implemented in any existing LBM code with just a few changes.

We have demonstrated that the oscillatory pattern of the LBM in the vicinity of shocks is not due to a lack of artificial diffusivity and are not pertinent to proper lattice Boltzmann schemes. On the other hand, there exists a Gibbs effect that we cannot fully suppress without artificial viscosity or special ad hoc approximation schemes.

The role of Gauss-Hermite quadratures in LBM constructions is now overestimated (here we fully agree with [4]). Other quadratures require slightly more points for the same degree of accuracy, but can be realised on integer nodes (and, more generally, are flexible with regards to the choice of nodes), which is more convenient for LBM needs.

The five-velocity lattice $\{0, \pm 1, \pm 2\}$ can produce a stable LBGK based method, as can many other “suspicious” lattices which were previously discussed by many authors as intrinsically unstable. These results can be immediately generalised onto high dimensional lattices (ND-lattices, cubatures and equilibria as products of 1D lattices, quadratures and equilibria). Finally, with the advent of stable multispeed lattice formulations comes the prospect of stable nonisothermic LBM realisations.

Acknowledgements

This work is supported by Engineering and Physical Sciences Research Council (EPSRC) grant number GR/S95572/01.

[1] S. Succi, *The lattice Boltzmann equation for fluid dynamics and beyond* (OUP, New York, 2001).
 [2] A. N. Gorban, in *Model Reduction and Coarse-Graining Approaches for Multiscale Phenomena* (Springer, Berlin-Heidelberg-New York, 2006), pp. 117–176, cond-mat/0602024.
 [3] P. J. Dellar, in *Computational Fluid and Solid Mechanics 2005* (Elsevier, Amsterdam, 2005), pp. 632–635.

[4] S. S. Chikatamarla and I. V. Karlin, Phys. Rev. Lett. **97**, 190601 (2006).
 [5] R. A. Brownlee, A. N. Gorban, and J. Levesley, Phys. Rev. E **74**, 037703 (2006).
 [6] R. A. Brownlee, A. N. Gorban, and J. Levesley, Phys. Rev. E (submitted) (2006), cond-mat/0611444.
 [7] A. N. Gorban and I. V. Karlin, Preprint IHES/P/03/57, Institut des Hautes Études Scientifiques, Bures-sur-

- Yvette, France (2003), cond-mat/0308331.
- [8] A. N. Gorban and I. V. Karlin, *Invariant manifolds for physical and chemical kinetics*, vol. 660 of *Lect. Notes Phys.* (Springer, Berlin-Heidelberg-New York, 2005).
 - [9] S. Ansumali and I. V. Karlin, *J. Stat. Phys.* **107**, 291 (2002).
 - [10] S. Ansumali and I. V. Karlin, *Phys. Rev. Lett.* **95**, 260605 (2005).
 - [11] X. He and L.-S. Luo, *Phys. Rev. E* **55**, R6333 (1997).
 - [12] X. Shan and X. He, *Phys. Rev. Lett.* **80**, 65 (1998).